Characteristics of turbulent flow behind detached rib in an adverse pressure gradient

A. M. El-Kersh
Mechanical Power and Energy Department, El-Minia University, Egypt

An experimental investigation on the characteristics of turbulent flow behind detached rib is carried out at inlet Reynolds number of 2.24 x 10^5. Effects of adverse pressure gradient (Clauser parameter = 0.0, 2.42 and 6.83) and clearance-to-rib height ratio (C/H=0.0, 0.4 and 2.0) on the length of recirculating region are examined. The results show that, the length of recirculating region increases with increasing adverse pressure gradient and decreasing clearance-to-rib height ratio. In general, the increase of adverse pressure gradient leads to increase the local Reynolds shear and normal stresses. These stresses exhibit maximum values at a height close to the height of upper edge of the rib and decreases in streamwise direction. Such decrease is more pronounced at lower pressure gradients. Furthermore, in zero pressure gradient the turbulent structure parameter in recirculating flow region is nearly close to that in attached flow and the presence of adverse pressure gradient significantly affect this structure at inner and outer layer regions. A detailed study on the calculations and selection of constant C_μ used in k-ε two equations model is presented.

الورقة تمثل بحث معملى على خصائص السريان خلف مضلع منفصل عن جدار السريان، وقد أجريت التجارب المعملية عند رقم رينولدز ٢,٢٤ x 10^5 وضغط متدرج مناوئ تم التعبير عنه برقم كلوزر عند صفر، ٢,٤٢ ، ٦,٨٣ وكانت قيم الخلوص بين المضلع وجدار السريان منسوبة إلى ارتفاع المضلع هى صفر ، ٠,٤٠ ، ٢,٠ . وقد أوضحت التجارب المعملية أن طول المنطقة الدوامية خلف المضلع يزداد بزيادة الضغط المتدرج المناوئ ومع نقص نسبة الخلوص إلى ارتفاع المضلع. وقد وجد أن زيادة الضغط المتدرج المناوئ يصاحبة زيادة فى اجهادات القص والإجهادات العمودية لرينولدز، كذلك فإن القيمة القصوى لإجهادات القص تنقص فى إتجاه السريان بمعدل أكبر عند الضغوط المناوئة المنخفضة، بالإضافة إلى ذلك فإن معامل هيكل الاضطراب متقارب فى المناطق الدوامية والمناطق التى أمامها فى إتجاه السريان عندما يكون الضغط المتدرج المناوئ يساوى صفراً، أما عند الضغوط الأعلى فإن معامل هيكل الاضطراب يتأثر تأثيراً واضحاً فىالمناطق الداخلية والخارجية للطبقة الجدارية، وقد تم عمل دراسة تفصيلية لحساب وإختيار الثابت C_μ والذى يستخدم فى النموذج الرياضى للسريان المضطرب والذى يعتمد على معادلتى طاقة الحركة للاضطراب وتبديد الطاقة.

Keywords: Detached rib, Pressure gradient, Turbulent flow, Reynolds stress, Boundary layers

1. Introduction

The problems of heat transfer characteristics and flow structure over a surface with artificial roughness elements have been considered in engineering applications by several research workers. Typical examples include the selection of size, shape and relative arrangements in rectangular channels [1-4], annular pipes [5], cooling panels of ramjet [6] and gas turbine blades [7]. The flow pattern past repeated solid ribs attached to the duct wall indicated that the increase of pitch-to-height ratio leads to reduce the length of recirculating zone behind the ribs. Furthermore, the ribbed ducts have to be operated at lower Reynolds number than the smooth ones to achieve equal pumping power [4]. Other studies for this type of flow configuration showed local deterioration of heat transfer in the near concave corners [2, 8]. The studies of heat transfer in the perforated [9] and detached [10] ribbed duct flows demonstrated better thermal performance compared with solid ribbed duct flows. In Low-aspect-ratio rectangular channel with perforated ribs, Liou et al. [3] showed that a staggered arrangement of the ribs gives almost the same friction and heat transfer results as symmetric ones. This trend is similar to that of the solid-type ribbed case obtained in their previous work [11]. Due to manufacturing concern towards the applications of perforated ribs, the detached ribs positioned at small height from the wall

have been recommended by Liou and Wang [12]. The detached ribs are surveyed by Liou et al. [10] who demonstrated that a vortex shedding occurs when the clearance between the cylinder and the wall is greater than a critical value. This critical clearance has typical values of 0.25-0.30, 0.35 and 0.35-0.50 times characteristic length of circular cylinder, triangular cylinder and square cylinder respectively. Their experimental results for rib detached-distance to rib-height ratios varied from zero to 3.25 showed that the peak local Nusselt number depends mainly on the dominant fluid dynamic factors.

The above relevant studies have reported valuable information related to the flow behavior and heat transfer due to attached and detached ribbed duct flows. Few experimental studies have been presented on flow structure downstream of detached ribs and these are limited to zero pressure gradients. However, in some practical applications the fluid flow systems are subjected to pressure gradients. In addition, information regarding the structure of turbulence in the recirculating region behind the detached ribs is not fully documented.

The object of the present investigation is to study the structure of turbulent flow past square detached rib in an adverse pressure gradient. The measurements of velocities, Reynolds shear and normal stresses have been carried out to understand this structure and to assess the accuracy of constant C_μ used in k-ε turbulence model.

2. Experimental arrangements

All experiments have been conducted in the low speed wind tunnel. The test section has a cross-section of 305 x 305 mm with a length of 600 mm and its roof is assembled with clamps to the test section. The adverse pressure gradient is developed by mounting a wedge to the roof of the test section as shown in fig. 1. Two wedges of 4 and 8 degs. are introduced to have two cases of adverse pressure gradients. A two-dimensional rib of 15 x 15 mm cross- section is mounted in the floor of the test section at a distance of 200 mm from the throat of the divergent section.

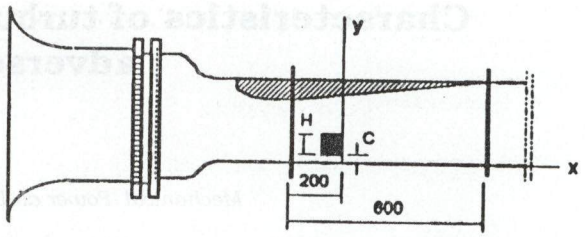

Fig. 1. Layout of the experimental arrangement.

Detailed measurements have been conducted at zero and adverse pressure gradients for the case of 6 mm clearance between the rib and floor of the test section which is equivalent to a clearance-to-rib height ratio C/H of 0.4. This configuration is considered because it represents the limits between the rapid and slower decrease from the reattached wake flow to the free wake flow for single [23, 24] and multi-ribs [10]. In addition, subsequent measurements are carried out for C/H=0.0 and 2.0 to detect the length of recirculating zone downstream of the rib.

The hot wire anemometer at constant temperature is used for the velocity and turbulence measurements at five axial stations located at the central plane of the test section downstream of the rib. Measurements are made with straight and 45° slant probe elements using the same technique as that described by Ng [13]. The slant wire was presented at an angle of 45° to the direction of flow and rotated through 360° in 90° intervals. This facility, in combination with the straight wire readings allowed the turbulence parameters to be calculated. All probes are calibrated in the free stream of wind tunnel against a standard pitot static tube.

All measurements are conducted at inlet Reynolds Number (Re_i) of 2.24 x 10^5. Preliminary measurements regarding the static pressure gradient and the boundary layer velocities are carried out along the floor of the test section without rib. The pressure gradients at the location of the rib with zero, 4 and 8 degs. wedge angles in terms of Clauser parameter β are 0.0, 2.42 and 6.83 with a corresponding boundary layers shape factors (S) of 1.356, 1.442 and 1.529, respectively. The uncertainty of the measured quantities U,

u'^2, v'^2 and $u'v'$ are less than 2.4, 3.6, 8.4 and 4.3 percent, respectively.

3. Results and discution

3.1 Time-mean velocity profiles

The axial mean velocity profiles for the cases of Clauser parameter β = 0.0, 2.42 and 6.83 are shown in figs. 2-a, 2-b and 2-c. It is seen that the boundary layer thickness tends to increase with increasing pressure gradient. In addition, all cases present a maximum negative velocity at x/H=1.0 which increases with increasing the adverse pressure gradient. In addition, the wake behind the rib tends to decay slower at higher pressure gradient leading to increase the recirculating flow region. This region is presented in figs. 3-a, 3-b and 3-c by drawing the iso-velocity contours. It is seen that, the size of recirculating flow region increases with increasing pressure gradient. Furthermore, the axial recirculating length at which the negative wake velocity diminishes increases from 2.3 to 4.5 rib heights as the Clauser parameter increases from 0.0 to 6.83.

The axial velocity variation along the symmetric axis of the rib in x –direction (x/H=0.9) is shown in fig. 4. It is clear that the tendency of flow velocity to change from negative to positive value is faster at lower pressure gradient. This in turn leads to reduce the flow recovery zone downstream of recirculating region. The axial velocity distribution very near to the wall at y/H=0.1 is shown in fig. 5. The velocity is remarkably decreased as x/H increases from 1.0 to 3.0 and in particular at lower pressure gradients.

The effect of rib clearance on the length of recirculating region is shown in fig. 6. It is seen that the length of wake or recirculating region increases with increasing the pressure gradient and decreasing the clearance to rib height ratio. It may be considered that the wakes decay or growth depends on the relative magnitude of the pressure and shear stresses, and for adverse pressure gradient the wakes tend to grow rather than decay [14]. Furthermore, the recirculating region is substantially decreases with increasing C/H up to 0.4 and less reduction is present for C/H greater than 0.4.

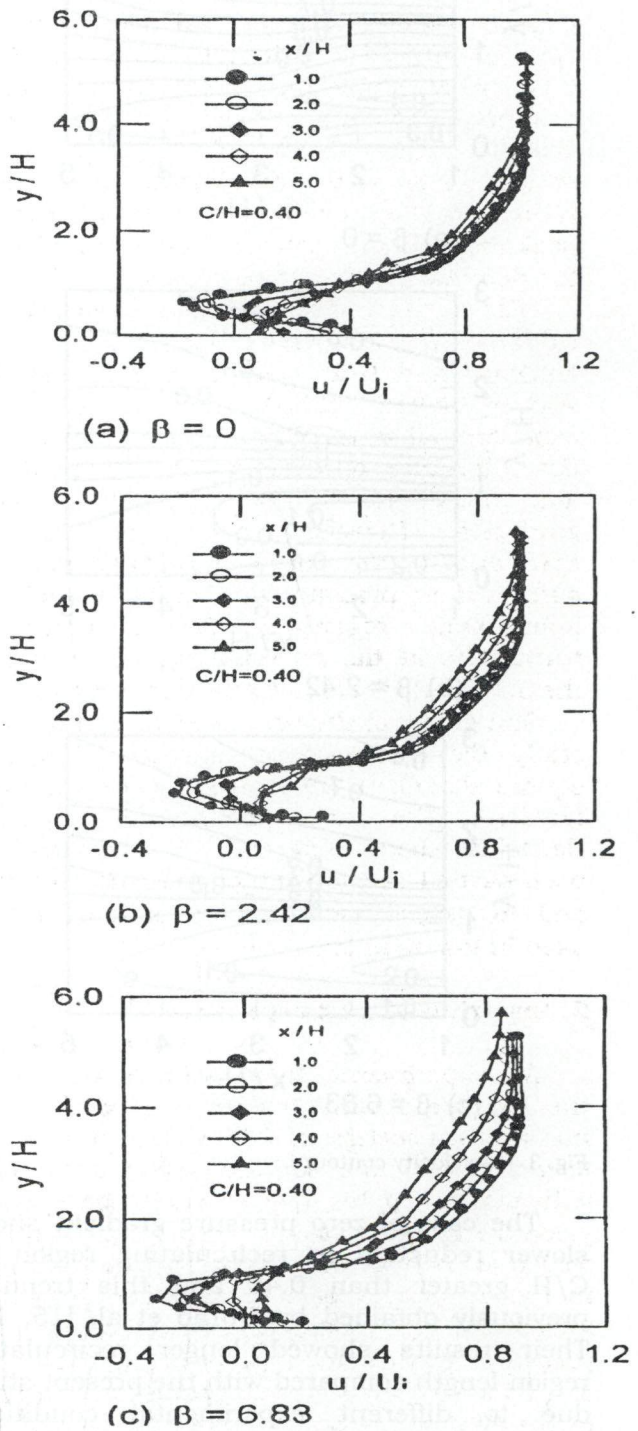

Fig. 2. Alxial velocity profiles.

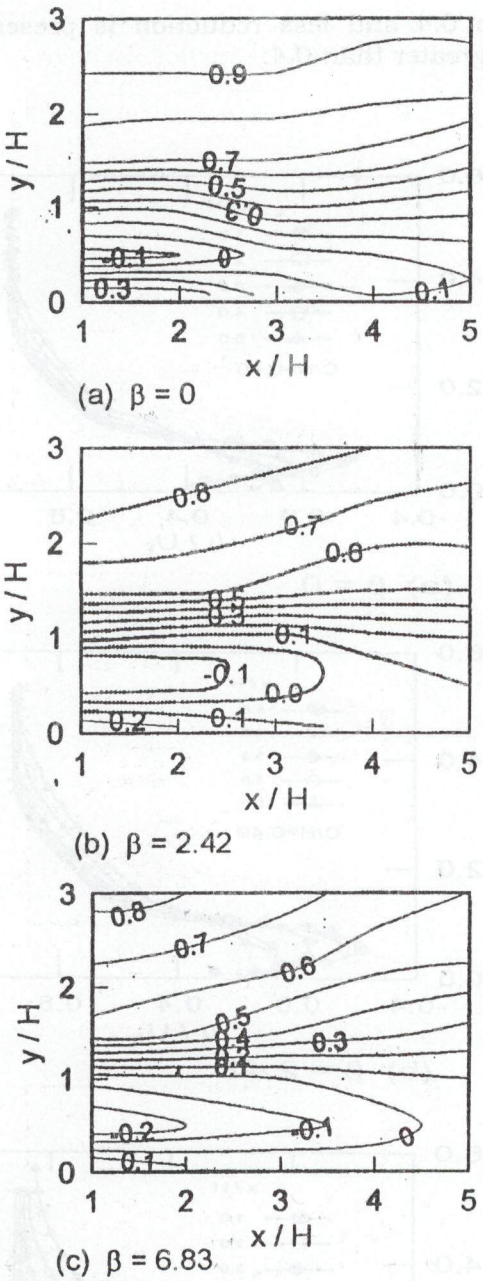

Fig. 3. Iso-velocity contours.

The case of zero pressure gradient shows slower reduction in recirculating region for C/H greater than 0.40 and this trend is previously obtained by Durao et al. [15, 16]. Their results showed longer recirculating region length compared with the present study due to different experimental conditions regarding turbulence level, inlet Reynolds number and the ratio between the rib height and channel hydraulic diameter. The experiments of Durao et al. [15, 16] have been carried out with fully developed flow at $Re_i = 1.36 \times 10^4$ and $H/D_h = 0.147$.

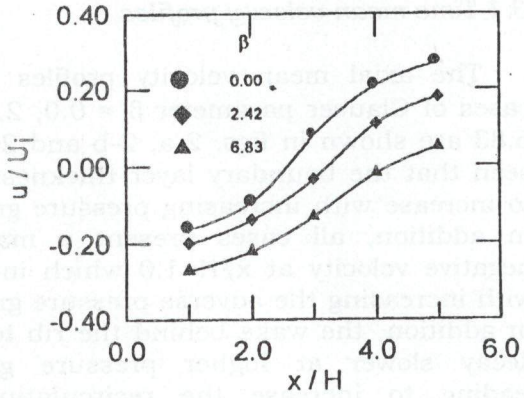

Fig. 4. Axial velocity distributions at y/H=0.90 for C/H=0.40.

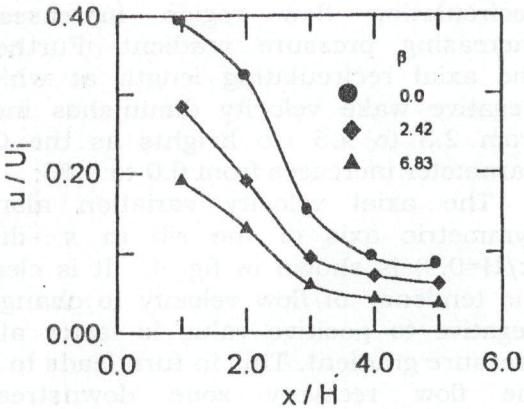

Fig. 5. Axial velocity distributions at y/H=0.10 for C/H=0.40.

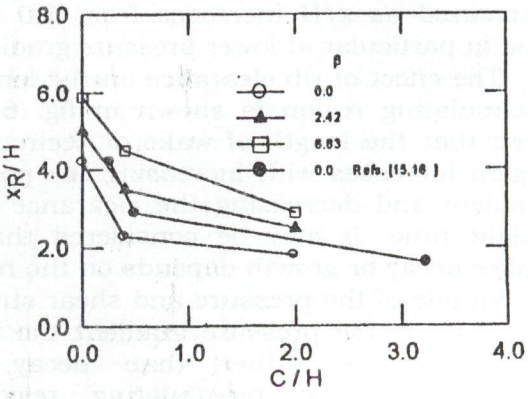

Fig. 6. Effect of rib clearance on the length of recirculating region.

3.2. Reynolds shear and normal stresses

Because the turbulence model depends on the expressions of Reynolds shear and normal stresses, therefor they are presented in this work. Reynolds shear stress profiles downstream of the rib are shown in figs. 7-a, 7-b and 7-c. The measured peak value occurs at y/H close to 1.4. This is attributed to the maximum velocity gradient downstream of the rib upper edge. The profiles indicate that the application of adverse pressure gradient prohibits the diffusive behavior of the wake and increases the shear stress. The increase of shear stress at the outer layers with pressure gradient is also observed. Consequently, this considerable energy production due to Reynolds shear stress affects the development of the inner layer. The distribution of maximum Reynolds shear stress downstream of detached rib is shown in fig. 8. It is seen that, the shear stress decreases with increasing axial distance in streamwise direction. The results at zero pressure gradient agree with the findings of Liou et al. [10]. In addition, the reduction of shear stress with axial length is more pronounced as the pressure gradient decreases leading to faster flow recovery downstream of recirculating region.

The Reynolds normal stress profiles increase with increasing pressure gradient as shown in figs. 9-a, b and 9-c. The variation of Reynolds normal stress with axial distance near the boundary layer edge is slightly affected for the case of zero pressure gradient. However, significant increases in normal stresses occur near the boundary layer edge at higher pressure gradient. As expected the measurements showed that the longitudinal turbulence intensity is larger than the transverse intensity and in particular behind the upper edge of the rib, which indicates that the flow is anisotropy.

3.3. Turbulent structure parameter

The turbulent structure parameter is defined by the ratio between the shear stress and turbulent kinetic energy and the following section discuss the calculation of this parameter from the measurements and its importance in the turbulence modeling.

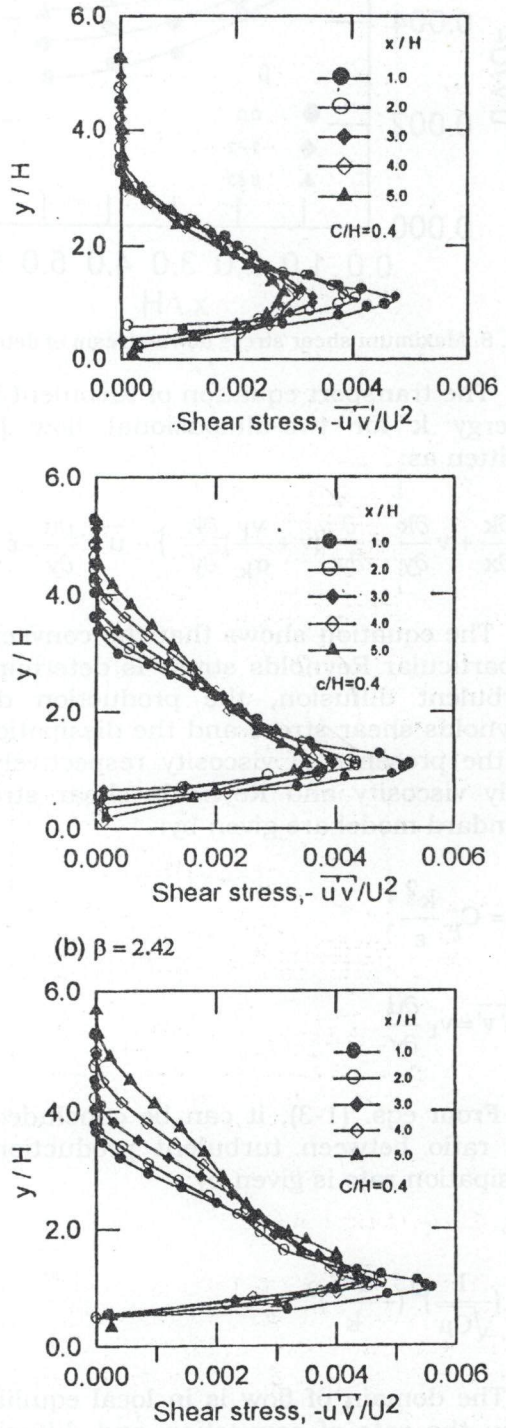

Fig. 7. Shear stress profiles.

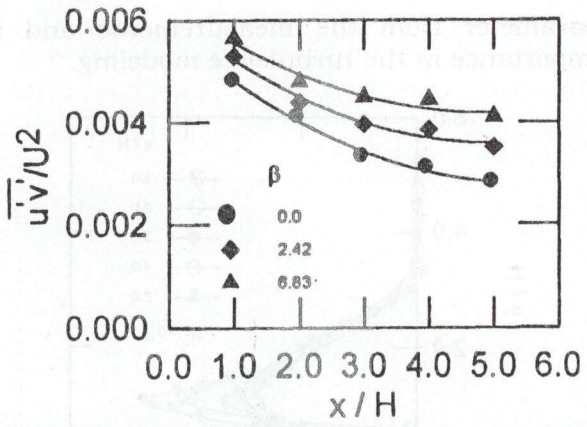

Fig. 8. Maximum shear stress down-stream of detched rib.

The transport equation of turbulent kinetic energy k for two-dimensional flow [17] is written as:

$$u\frac{\partial k}{\partial x}+v\frac{\partial k}{\partial y}=\frac{\partial}{\partial y}\{(\nu+\frac{\nu_t}{\sigma_k})\frac{\partial k}{\partial y}\}-\overline{u'v'}\frac{\partial u}{\partial y}-\varepsilon\,. \quad (1)$$

The equation shows that the convection of a particular Reynolds stress is determined by turbulent diffusion, the production due to Reynolds shear stress and the dissipation due to the presence of viscosity respectively. The eddy viscosity and Reynolds shear stress in standard model are given by:

$$\nu_t = C_\mu \frac{k^2}{\varepsilon}, \quad (2)$$

$$-\overline{u'v'}=\nu_t\frac{\partial u}{\partial y} \quad (3)$$

From eqs. (1-3), it can be concluded that the ratio between turbulent production and dissipation rate is given by:

$$R=(\frac{1}{\sqrt{C\mu}})^2(-\frac{\overline{u'v'}}{k})^2\,. \quad (4)$$

The domain of flow is in local equilibrium when the rate of convection and diffusion of turbulent kinetic energy is negligible compared with the rate of

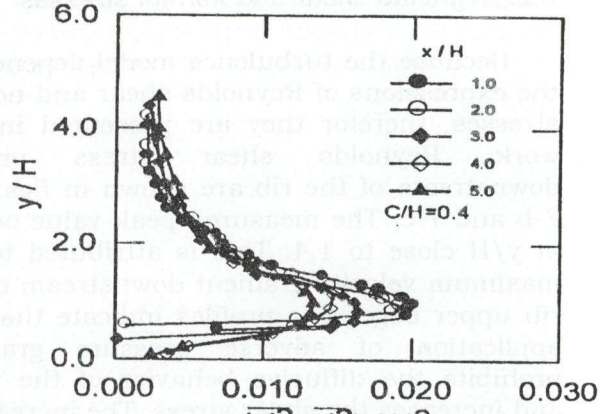

(a) β=0.0

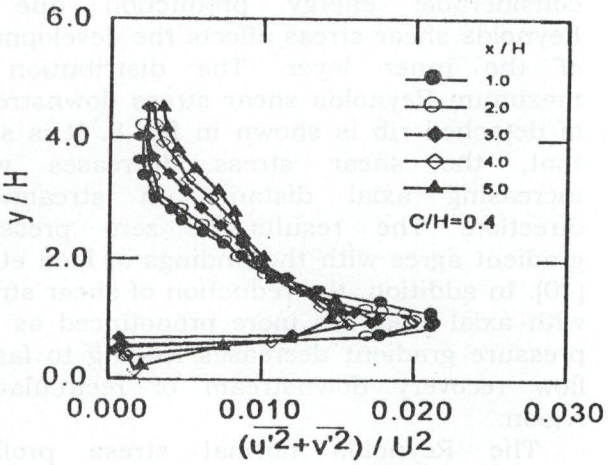

(b) β = 2.42

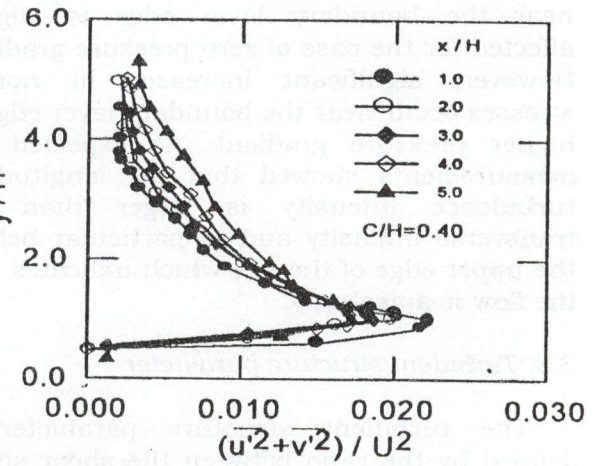

(c) β = 6.83

Fig. 9. Reynlds normal steresses.

production and dissipation. Consequently the turbulent generation and dissipation are equal (R=1) and leads to the following relation of structure parameter:

$$-\frac{\overline{u'v'}}{k} = \sqrt{C_\mu} \cdot \qquad (5)$$

In the standard k-ε model, the value of C_μ is 0.09. However, Nangen et al. [18] demonstrates that, there is no rigorous basis to select C_μ equal to 0.09, and this is one of reasons to cause the difference between the computed values and the experimental data in some flow field, especially for Reynolds stress. Because the flow field in most engineering applications is not in local equilibrium, some research workers suggested different model functions to account for the near wall effects on the C_μ [18-21]. However, these expressions are limited to specific flow fields. In complex flow fields, some research workers explained the deviation between the experimental results and the theoretical model to the lack of accurate value C_μ. Therefore, it is better to calculate this value from the data of experimental measurements in order to assess the theoretical model. Liou et al. [10] showed that, because of different degrees of flow complexity, the calculated constant C_μ from the measured Reynolds shear stress and kinetic energy of detached rib differs from that in jets, wakes and boundary layer as surveyed by Harsha and Lee [21].

In the present analysis, the variation of turbulent structure parameter ($-\overline{u'v'}/k$) across the boundary layers at different pressure gradients are shown in figs. 10-a and 10-b. In zero pressure gradient, It is seen that the structure parameter in separating flow is nearly close to that in attached flows within the experimental error. This is in agreement with the findings of Avva et al. [22] for backward-facing step flow. The presence of pressure gradient leads to increase the structure parameter at the inner layers, whereas the opposite effect occurs at the outer layers. This is attributed to the deviation of flow from anisotropy due to increase pressure gradient. In addition, the present results at zero pressure gradients are compared with the experimental work of other research workers as shown in fig. 10-a. Each curve is obtained from the data of shear stress and turbulent kinetic

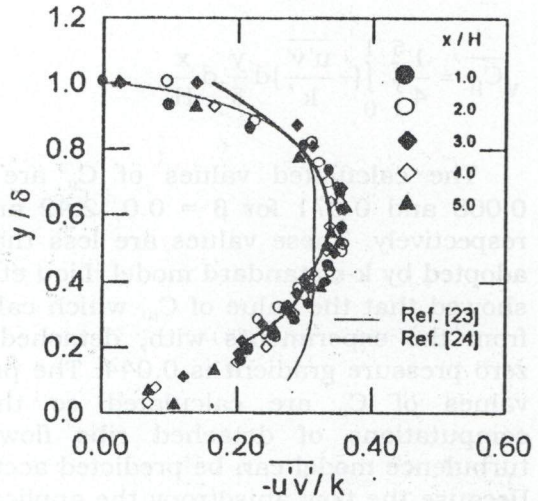

Fig. 10-a. Variation of-uv/k acros boundary layers for β=0.0.

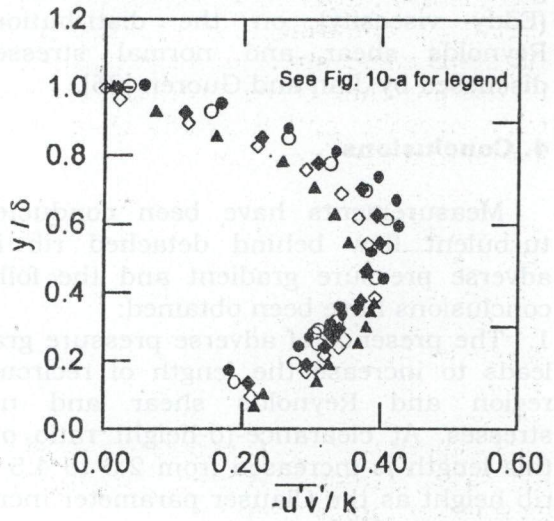

Fig. 10-b. Variation of-uv/k acros boundary layers for β=6.83.

energy presented by research workers. It is seen that, the fully developed pipe flow [23] as presented by Ng [13] and the flow over a backward–facing step [25] have different distributions and the later shows better agreement with the present experimental results. This is attributed to the nature of flow field between the present flow and the flow downstream of backward step with

recirculating region. In the present work the value of C_μ is calculated by averaging the turbulent structure over the domain of measurements using the following relation:

$$\sqrt{C_\mu} = \frac{1}{4}\int_1^5 \int_0^1 (-\frac{\overline{u'v'}}{k}) d\frac{y}{\delta}\, d\frac{x}{H}. \qquad (6)$$

The calculated values of C_μ are 0.056, 0.068 and 0.071 for β = 0.0, 2.42 and 6.83 respectively. These values are less than 0.09 adopted by k-ε standard model. Liou et al. [10] showed that the value of C_μ, which calculated from the experiments with, detached rib at zero pressure gradient is 0.044. The proposed values of C_μ are calculated so that the computations of detached ribs flow using turbulence model can be predicted accurately. Because the flow anisotropy the application of k-ε-S (Stochastic theory) model is recommended for such type of flow which gives substantial improvement over k-ε-E (Eddy viscosity) on the distributions of Reynolds shear and normal stresses as discussed by Jian and Guoren [25].

4. Conclusions

Measurements have been conducted on turbulent flow behind detached rib in an adverse pressure gradient and the following conclusions have been obtained:

1. The presence of adverse pressure gradient leads to increase the length of recirculating region and Reynolds shear and normal stresses. At clearance-to-height ratio of 0.4, this length is increased from 2.3 to 4.5 times rib height as the Clauser parameter increases from zero to 6.83.
2. The length of recirculating region substantially decreases with increasing clearance-to-height rib C/H up to 0.4 and less reduction is present for C/H greater than 0.40 for zero and adverse pressure gradients.
3. The maximum shear stresses are found to occur downstream of trailing upper edge of the rib and decreases in streamwise direction.
4. The distribution of structure parameter is consistent in recirculating and detached flow regions at zero pressure gradient. However, it is increased in inner layers in streamwise direction and has the opposite effect at the outer layers in higher adverse pressure gradients.
5. The calculated values of constant C_μ used in k-ε two equations model are 0.056, 0.068 and 0.071 for Clauser parameter β of 0.0, 2.42 and 6.83, respectively compared with a value of 0.09 used in standard model.

Nomenclature

C is the clearance between wall and rib,
C_μ is the constant in the turbulence model,
D_h is the duct hydraulic diameter at inlet,
H is the rib height,
k is th turbulent kinetic energy,
p is the wall static pressure,
Re_i is the inlet Reynolds number, $U_b D_h/\nu$,
S is the boundary layer shape factor, δ^*/θ,
u is the time-mean velocity in x-direction,
u' is the instantaneous fluctuating component, of u U_b bulk mean velocity at inlet,
U is the time-mean axial velocity at the edge of boundary layer,
v is the time-mean velocity normal to the wall,
v' is the instantaneous fluctuating component of v,
x is the distance along the main flow direction,
y is the distance normal to x-direction,
β is the clauser parameter,, $\delta^*/\tau_w\, dp/dx$,
δ is the boundary layer thickness,
δ^* is the displacement thickness, $\int_0^\delta (1-\frac{u}{U})dy$,
ε is the rate of dissipation of turbulence energy,
θ is the boundary layer momentum thickness,
σ_k is the turbulent Prandtl number of k,
τ_w is the wall shear stress,
ν is the kinematic viscosity, and
ν_t is the turbulent kinematic viscosity.

References

[1] J. C. Han, and Y. M. Zhang, "High Performance Heat Transfer Ducts with Parallel Broken and V-Shaped Broken

Ribs", Int. J. Heat Transfer, Vol. 35 (2), pp. 513-523 (1992).

[2] T. M. Liou, and J. J. Hwang, "Effects of Ridge Shapes on Turbulent Heat Transfer and Friction in a Rectangular Channel", Int. J. Heat Mass Transfer, Vol. 36, pp. 931-940 (1993).

[3] J. J. Hwang, and T. M. Liou, "Heat Transfer and Friction in a Low-Aspect Ratio Rectangular Channel with Staggered Perforated Ribs on Two Opposite Walls", ASME Journal of Heat Transfer, Vol. 117, pp. 843-850 (1995).

[4] A. M. El-Kersh, "Flow Pattern Past Repeated Square Ribs in Rectangular Ducts", Bulletin of the Faculty of Engineering, Assiut University, Vol. 27 (1), pp. 101-109 (1999).

[5] B. K. Lee, N. H. Cho, and Y. D. Choi, "Analysis of Periodically Fully Developed Turbulent Flow and Heat Transfer by k-ε Equation Model in Artificially Roughened Annulus", Int. J. Heat Mass Transfer, Vol. 31 (9), pp. 1797-1806 (1988).

[6] B. H.Chang, and A. F. Mills "Turbulent Flow in a Channel with Transverse Rib Heat Transfer Augmentation", International Journal of Heat and Mass Transfer, Vol. 30 (6), pp. 1459-1469 (1993).

[7] M.W. Pinson, T. and Wang, "Effects of Leading Edge Roughness on Fluid Flow and Heat Transfer in the Transitional Boundary Layer Over a Flat Plate", International Journal of Heat and Mass Transfer, Vol. 40 (12), pp. 2813-2823 (1997).

[8] T. M. Liou, and J. J. Hwang, "Turbulent Heat Transfer Augmentation and Friction in Periodic Fully Developed Channel Flows" ASME Journal of Heat Transfer, Vol. 114, pp. 56-64 (1992).

[9] J. J. Hwang, and T. M. Liou, "Augmented Heat Transfer in a Rectangular Channel with Permeable Ribs Mounted on the Wall", ASME Journal of Heat Transfer, Vol. 116, pp. 890-897 (1994).

[10] T. M. Liou, C. P. Yang, and H. L. Lee, "LDV Measurements of Spatially Periodic Flows Over a Detached Solid-Rib Array", ASME Journal of Fluids Engineering, Vol. 119, pp. 383-389 (1997).

[11] J. J. Hwang, and T. M. Liou, "Effect of Permeable Ribs on Heat Transfer and Friction in a Rectangular Channel", ASME Journal of Turbomachinery, Vol. 117, pp. 265-271 (1995).

[12] T. M. Liou, and W. B. Wang, "Laser Interferometry Study of Developing Heat Transfer in a Duct with a Detached Rib Array", Int. J. Heat Mass Transfer, Vol. 38 (1), pp. 91-100 (1995).

[13] K. H. Ng, "Predictions of Turbulent Boundary –Layer Developments Using a Two-Equation Model of Turbulence", Ph.D. Thesis, Faculty of Engineering, University of London (1971).

[14] P. G. Hill, U. W. Schaub, and Y. Senoo, "Turbulent Wakes in Pressure Gradient", ASME Journal of Applied Mechanics, Paper No. 63-WA-5 .

[15] D. F. G. Durao, M. V. Heitor, and J. C. F. Pereira, "Measurements of Turbulent and Periodic Flows Around a square Cross-Section Cylinder", Experiments in Fluid, Vol. 6, pp. 298-304 (1988).

[16] D. F. G. Durao, P. S. T. Gouveia, and J. C. F. Pereira, "Velocity Characteristics of the Flow Around a Square Cross Section Cylinder Placed Near a Channel Wall", Experiments in Fluid, Vol. 11, pp. 341-350 (1991).

[17] T. Kondoh, K. Abe, and Y. Nagano,"A New Turbulence Model for Predicting Fluid Flow and Heat Transfer in Separating and Reattaching Flows-I. Flow Field Calculations", Int. J. Heat Mass Transfer, Vol. 37 (1), pp. 139-151 (1994).

[18] N. Hangen, C. Liang, and L. Shujun, "On the Expression for C_μ in k-ε Two Equations Turbulence Model", Flow Modeling and Turbulence Measurements, Hemisphere Pub. Co., pp. 92-99 (1992).

[19] T. Nagano, and M. Hishida, "Improved Form of the k-ε Model for Wall Turbulent Shear Flows", Trans. of ASME, Vol. 109, pp. 156-160 (1987).

[20] S. Ushijma, "Prediction of Temperature Fluctuation Near an Adiabatic Side Wall

in a Stratified Flow", Flow Modeling and Turbulence Measurements, Hemisphere Pub. Co., pp. 357-364 (1992).

[21] P. T. Harsha, and S. C. Lee, "Correlation between Turbulent Shear Stress and Turbulent Kinetic Energy", AIAA Journal, Vol. 8 (8), pp. 1508-1510, (1970).

[22] R. K. Avva, S. J. Kline, and , J. H. Ferziger "Computation of Turbulent Flow Over a Backward-Facing Step-Zonal Approach, AIAA-88-0611 (1988).

[23] J. Laufer, "The structure of Turbulence in a Fully Developed Pipe Flow", NACA Rep. 1174 (1954).

[24] Y. Jian, and D. Guoren, "The Investigation of k-ε-S Turbulence Model", Flow Modeling and Turbulence Measurements, Hemisphere Pub. Co., pp. 144-152 (1992).

Received January 9, 2001
Accepted May 13, 2001